

Real-time MR Imaging Controlled by Transperineal Needle Placement Device for MRI-guided Prostate Biopsy and Brachytherapy

J. Tokuda^{1,2}, S. DiMaio^{1,2}, G. Fischer³, C. Csoma³, D. Gobbi⁴, G. Fichtinger⁴, N. Hata^{1,2}, and C. Tempany^{1,2}

¹Department of Radiology, Brigham and Women's Hospital, Boston, MA, United States, ²Department of Radiology, Harvard Medical School, Boston, MA, United States, ³ERC CISST, The Johns Hopkins University, Baltimore, MD, United States, ⁴School of Computing, Queen's University, Kingston, Ontario, Canada

Introduction: MRI is an ideal guiding tool for prostate cancer biopsy and local therapy due to its high sensitivity and specificity to focal prostate lesions and its radiation safety. However, closed-bore high-field MR magnets, which provide better images than interventional magnets, allow only limited access to the patient, and this makes real-time monitoring of the delivery process difficult. To overcome this limitation and increase the merit of MRI-guided biopsy and brachytherapy, we have been developing a MRI-compatible needle placement robot for transperineal prostate biopsy and therapy [1] (Fig. 1). In this study, we focused on an integration of real-time MR imaging with the robot for "closed-loop" needle guidance, where the action made by the robot is captured by the MR image, and immediately fed back to physicians to aid their a decision for the next action. Our proposed integration strategy is to use open-source visualization and communication tools, which enable real-time imaging plane control according to the needle position, as measured by the encoders of the robot, was developed. By rapidly imaging in planes that are parallel or perpendicular to the needle, a physician can monitor needle advancement in the tissue through MR images in real-time and interactively correct the needle path.

Methods: The system consisted of three major components: the needle placement robot, a closed-bore whole body 3T MRI scanner (GE Excite HD 3T, GE Healthcare, UK), and open-source surgical navigation software (3D Slicer, <http://www.slicer.org/>) running on a Linux-based workstation (SunJava Workstation W2100z, Sun Microsystems, CA). All components were connected to each other via 100Base-T Ethernet. NaviTrack, an open-source library for device connection and communication [2] was used to exchange various types of data including commands, positional data, and images among the components (Fig. 2). To register the coordinate systems of the robot and the MRI scanner, a Z-shaped fiducial frame [3] was attached to the robot. The position and orientation of the Z-shaped frame in image coordinate system can be determined by a single sectional image, and therefore coordinate transformation between the scanner and the robot can be established. Once this is done, the needle position and orientation measured by the encoders of the robot can be transferred to the MR image coordinate system for display on the surgical navigation workstation. This occurs every 100 ms to show the current needle position on the image (Fig. 3). At the same time, the navigation software sends the desired position and orientation of the needle to the robot, and also sends the desired position and orientation of the scan plane to the scanner to keep the imaging plane parallel (or perpendicular) to the needle throughout the procedure. The scan data is immediately transferred to the navigation software, where it is reconstructed and displayed.

Experiments: To test the performance of the system, the latency and positional accuracy of the real-time imaging were evaluated using a phantom. In this study, we connected the scanner and the navigation software to a robot simulator, which receives the target position and returns exactly the same position to the navigation software as a current virtual needle position, in order to exclude the mechanical error of the robot. The orientation of the virtual needle was fixed along the static magnetic field to simulate the transperineum biopsy/brachytherapy case. The phantom, in which 24 markers were embedded at know positions in 20×20×20 cm space, was placed in the gantry of the scanner. The Z-shaped frame was attached to the phantom to register the marker positions to the MR image coordinates. The position of each marker was calculated after the calibration. Note that the marker positions represented in the MR image coordinate system involved errors due to the registration, and therefore the overall error of the real-time image was quantified by comparison with the positions of the imaged markers. A 2D spoiled gradient recalled (SPGR) sequence was used for 2D real-time imaging with following parameters: matrix = 256×256; FOV = 30 mm; slice thickness = 5mm; flip angle = 30 deg. To vary the frame rate of the image, TR/TE were set to 12.8/6.2ms (3.3 s/frame), 15.2/5.1ms (3.9 s/frame) and 18.6/5.0ms (4.8 s/frame). To quantify the position error of the 2D images, each marker was specified as the virtual needle tip, and three orthogonal planes are acquired. A 3D image was also acquired prior to the real-time imaging as a reference. The parameters for the 3D image were: matrix = 256×256×72; FOV = 30 mm; slice thickness = 2mm; TR/TE = 6.3/2.1ms; flip angle = 30 deg. For the latency evaluation, the virtual needle tip was reciprocated with a range of 100 mm and a duration of 20 s during imaging the phantom. 120 images were recorded to the storage of the workstation with time stamps for each frame. Since the center of the image follows the virtual needle tip, delay of the real-time image was quantified by measuring the motion of the phantom in the image.

Results: The real-time 2D images were successfully acquired in three orthogonal planes parallel and perpendicular to the simulated needle, and visualized on the navigation software. The latencies of visualization of the real-time image on the navigation software for each frame rate were 5.0 s (3.3 s/frame), 5.6 s (3.9 s/frame) and 6.5 s (4.8 s/frame), since the navigation software received the needle position from the robot. Standard deviations of the latencies were 0.06-0.07 s in all cases. The root mean square errors between the specified target position and imaged target were 4.8 mm for 3D and 3.7 mm for 2D real-time images.

Discussion and Conclusion: It was feasible to integrate the scanner, navigation software and the robot using open-source software tools. The performance evaluation showed that the integrated system provided real-time visualization of 2D image parallel or perpendicular to the needle with enough accuracy for prostate biopsy and brachytherapy, where 5 mm positioning accuracy is required. The positional accuracy was degraded in the outer area of the phantom, because of the field inhomogeneity. Distortion correction after image reconstruction could be effective to improve the accuracy. The frame rate and latency of the real-time image affect needle advancement speed, and therefore interactivity of the guidance. It is possible to decreased the latency to approx. 3 s by using faster imaging sequence with frame rate of near 1 frame/s, since the latency study indicates that the latency due to the system (data transfer and image reconstruction) was 1.7 s.

Acknowledgements: This work is supported by NIH Grant 1R01CA111288.

References: [1] Fischer GS et al, Proc. MICCAI 2007; LNCS 4791:425-432; [2] Von Spiczak J et al, Stud Health Technol Inform 2007; 125:482-484; [3] DiMaio SP et. al, Proc. MICCAI 2007; LNCS 4792:50-58.

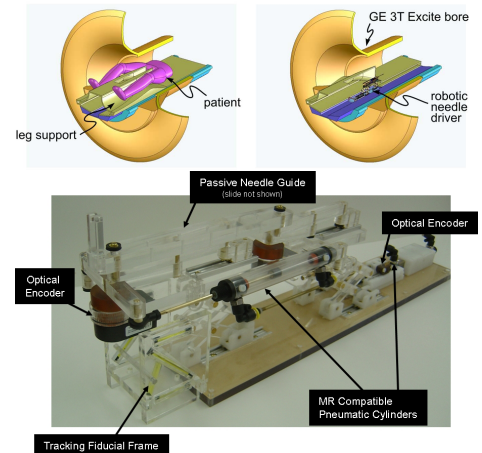


Fig. 1 A robot for transperineal prostate biopsy and treatment [1]. Pneumatic actuators and optical encoders are used for MRI-compatibility. Z-shaped fiducial frame was attached for a calibration.

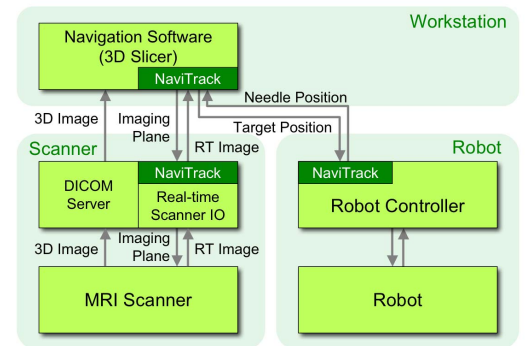


Fig. 2: System diagram for the robot for transperineal prostate biopsy and brachytherapy.

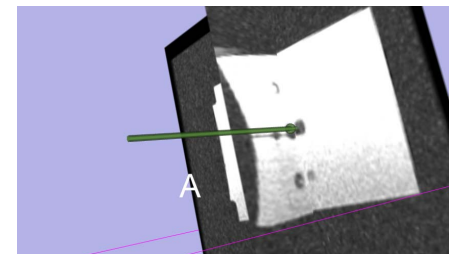


Fig. 3 Screenshot of 3D viewer on the navigation software 3D Slicer during needle insertion test with the robot.